Experimental photonic generation of chirped pulses using nonlinear dispersion-based incoherent processing

Manuel Rius, Mario Bolea, José Mora, Beatriz Ortega, and José Capmany

Abstract: We experimentally demonstrate, for the first time, a chirped microwave pulses generator based on the processing of an incoherent optical signal by means of a nonlinear dispersive element. Different capabilities have been demonstrated such as the control of the time-bandwidth product and the frequency tuning increasing the flexibility of the generated waveform compared to coherent techniques. Moreover, the use of differential detection improves considerably the limitation over the signal-to-noise ratio related to incoherent processing.

References and links

1. J. Yao, "Microwave photonics: arbitrary waveform generation," Nat. Photonics **4**(2), 79–80 (2010).
2. M. Li, J. Azaña, N. H. Zhu, and J. P. Yao, "Recent progresses on optical arbitrary waveform generation," Front. Optoelectron. **7**(3), 359–375 (2014).
3. J. Capmany and D. Novak, "Microwave photonics combines two worlds," Nat. Photonics **1**(6), 319–330 (2007).
4. J. Wang, H. Shen, L. Fan, R. Wu, B. Niu, L. T. Varghese, Y. Xuan, D. E. Leaird, X. Wang, F. Gan, A. M. Weiner, and M. Qi, "Reconfigurable radio-frequency arbitrary waveforms synthesized in a silicon photonic chip," Nat. Commun. **6**, 5957 (2015).
5. L. Maleki, "Sources: The optoelectronic oscillator," Nat. Photonics **5**(12), 728–730 (2011).
6. A. B. Matsko, L. Maleki, A. A. Savchenkov, and V. S. Ilchenko, "Whispering gallery mode based optoelectronic microwave oscillator," J. Mod. Opt. **50**(15-17), 2523–2542 (2003).
7. M. Bolea, J. Mora, B. Ortega, and J. Capmany, "Photonic arbitrary waveform generation applicable to multiband UWB communications," Opt. Express **18**(25), 26259–26267 (2010).
8. M. J. Zhang, T. G. Liu, A. B. Wang, J. Y. Zheng, L. N. Meng, Z. X. Zhang, and Y. C. Wang, "Photonic ultrawideband signal generator using an optically injected chaotic semiconductor laser," Opt. Lett. **36**(6), 1008–1010 (2011).
9. J. G. Proakis, *Digital Communications* (McGraw-Hill, 1995, *1*)
10. M. Skolnik, *Radar Handbook* (McGraw-Hill, 2008, *1*).
11. M. Bertero, M. Miyakawa, P. Boccacci, F. Conte, K. Orikasa, and M. Furutani, "Image restoration in chirp-pulse microwave CT (CP-MCT)," IEEE Trans. Biomed. Eng. **47**(5), 690–699 (2000).
12. M. Li, C. Wang, W. Li, and J. Yao, "An unbalanced temporal pulse shaping system for chirped microwave waveform generation," IEEE Trans. Microw. Theory Tech. **58**(11), 2968–2975 (2010).
13. H. Chi and J. Yao, "Chirped RF pulse generation based on optical spectral shaping and wavelength-to-time mapping using a nonlinearly chirped fiber Bragg grating," J. Lightwave Technol. **26**(10), 1282–1287 (2008).
14. C. Wang and J. Yao, "Photonic generation of chirped millimeter-wave pulses based on nonlinear frequency-to-time mapping in a nonlinearly chirped fiber Bragg grating," IEEE Trans. Microw. Theory Tech. **56**(2), 542–553 (2008).
15. H. Chi and J. Yao, "All-fiber chirped microwave pulses generation based on spectral shaping and wavelength-to-time conversion," IEEE Trans. Microw. Theory Tech. **55**(9), 1958–1963 (2007).
16. C. Wang and J. Yao, "Large Time-Bandwidth product microwave arbitrary waveform generation using a spatially chirped fiber Bragg grating," J. Lightwave Technol. **28**(11), 1652–1660 (2010).
17. C. Wang and J. Yao, "Chirped microwave pulse generation based on optical spectral shaping and wavelength-to-time mapping using a Sagnac-loop mirror incorporating a chirped fiber Bragg grating," J. Lightwave Technol. **27**(16), 3336–3341 (2009).

18. M. Li and J. P. Yao, "Photonic generation of continuously tunable chirped microwave waveforms based on a temporal interferometer incorporating an optically-pumped linearly-chirped fiber Bragg grating," IEEE Trans. Microw. Theory Tech. **59**(12), 3531–3537 (2011).
19. M. Bolea, J. Mora, B. Ortega, and J. Capmany, "Nonlinear dispersion-based incoherent photonic processing for microwave pulse generation with full reconfigurability," Opt. Express **20**(6), 6728–6736 (2012).
20. C. Dorrer, "Statistical analysis of incoherent pulse shaping," Opt. Express **17**(5), 3341–3352 (2009).
21. Y. Park and J. Azaña, "Ultrahigh dispersion of broadband microwave signals by incoherent photonic processing," Opt. Express **18**(14), 14752–14761 (2010).

1. Introduction

Photonic generation of microwave/millimeter-wave signals has been a field of interest in the last years due to its important impact on applications such as radar systems, wireless communications, medical image processing, software defined radio or modern instrumentation where high frequency and large bandwidth signals are required [1, 2]. The use of microwave photonics (MWP) technology in microwave signal generation offers new features and improved performance related to the inherent advantages of operating in the optical domain such as low losses, high bandwidth, immunity to electromagnetic interference (EMI) and, especially in this case, also the possibility of tuning and reconfiguration [3, 4].

Different techniques have been developed to generate a wide variety of signals using schemes from a single electronic oscillator to an arbitrary waveform generator. For instance, high spectral purity microwave signals can be generated without a reference microwave signal by means of opto-electronic oscillators (OEO) [5, 6]. Besides, other signals such as ultra-wideband (UWB) can be achieved by means of more flexible schemes including MWP arbitrary waveform generators [7, 8]. More specifically, one of these interesting signals is the chirped microwave pulse with the main characteristic of having a frequency variation along the time duration pulse, which involves a large bandwidth signal processing. Among the diverse applications where chirped microwave pulses are used, spread spectrum communications, pulsed compression radars or tomography for medical imaging [9–11] can be highlighted.

In order to compare chirped microwave pulses Time-Bandwidth Product (TBWP) parameter is defined as the product of the full-width time duration of the pulse at half-maximum (T_{FWHM}) and the differential value of its frequency variation. In this context, approaches based on different photonic techniques to generate chirped microwave pulses have been reported. By means of unbalanced temporal pulse-shaping technique a TBWP of 3 can be obtained [12]. A TBWP around 4 is achieved using a frequency-to-time mapping in a nonlinearly chirped FBG (NLCFBG) [13, 14] or dispersive fiber [15]. Introducing an optical spectral shaping and wavelength-to-time mapping using spatially chirped fiber Bragg grating [16], a Sagnac-loop mirror incorporating a chirped fiber Bragg grating [17] or an interferometric structure incorporating an optically-pumped linearly chirped fiber Bragg grating [18], the TBWP can be increased up to 23, 40 and 45, respectively. All previous schemes are based on a coherent technique with a limiting flexibility to reconfigure the output waveform which is determining for applications such as radar pulse compression [10]. In order to overcome this lack of flexibility, we recently proposed a photonic scheme which theoretically permits to increase the chirped waveform flexibility compared with coherent techniques by means of incoherent processing using a nonlinear dispersive element [19].

In this context, we experimentally evaluate the incoherent technique for generating chirped pulses using an all optical tunable single-bandpass microwave photonic filter as we propose theoretically in [19]. In principle, the use of incoherent light processing leads to lower signal-to-noise ratio (SNR) than using coherent techniques [20]. However, an improvement of the SNR is achieved due to the use of differential detection in the experimental scheme besides the use of adaptative average [21]. From the previous theoretical analysis [19], we adapt that discussion to this proposal. We demonstrate an independent control of the TBWP through the dispersion of the system and also an independent control of

the central frequency of the generated signal through the adjustment of the processing stage. Moreover, a TBWP value of 26.4 is achieved, which is roughly in the same order of magnitude than obtained by coherent techniques and increasing considerably the waveform flexibility. Therefore, our approach permits to exploit the capacity of obtaining high TBWP values similar to coherent techniques. Additionally, our proposal offers waveform reconfigurability with an independent control of signal characteristics such as central frequency and chirp.

2. System description

The experimental setup of the proposed chirped microwave pulse generator is shown in Fig. 1. The operation principle of this structure can be analyzed in terms of incoherent signal processing by means of nonlinear dispersion [19]. In this case, our experimental scheme takes advantage of the differential detection unlike the previous theoretical proposal.

The optical source is composed by a Broadband Source (BBS) and an Optical Channel Selector (OCS). The BBS has a total optical bandwidth of 80 nm and the OCS is centered at 1546.92 nm with 48 channels of 0.8 nm width which attenuation can be controlled independently to achieve different optical power distributions. The optical signal is launched into a Mach-Zehnder Modulator (MZM) (Avanex SD40) to be modulated by a Radio Frequency (RF) pulse, $p_{RF}(t)$, coming from an electrical signal generator. The 3-dB bandwidth of MZM is 30 GHz. The electrical generator is configured at a bit rate of 12.5 Gbps with a pattern of one "1" and two hundred and fifty-five "0". Therefore, the repetition rate is close to 48.8 MHz and the pulse width is 80 ps. The modulated optical signal propagates through a single mode fiber (SMF-28) link of length L. In this case, the fiber link is considered as a non-linear dispersive element with the following dispersive parameters: $\beta_2 = -22$ ps^2/km and $\beta_3 = 0.14$ ps^3/km at 1550 nm. After the fiber link, a Mach-Zehnder Interferometer (MZI) is located in the system composed by two 50/50 optical couplers with ports 1x2 and 2x2 and a Variable Delay Line (VDL) for controlling the time delay ($\Delta\tau$) between both arms. In this case, the optical power between both arms has been balanced in order to maximize the transfer function of the MZI. Finally, the two complementary outputs of the MZI are connected to the input ports of a Balanced Photodetector (BPD) (u2t BPDV2020R-VF-FP) with a 3-dB bandwidth of 40 GHz which provides the electrical output of the system as a result of the difference between both detected optical signals. A 26.5 GHz bandwidth spectrum analyzer (Agilent N9020A) and a 50 GHz sampling oscilloscope (Tektronix DSA8200) are used to measure the generated RF spectrum and waveform, respectively.
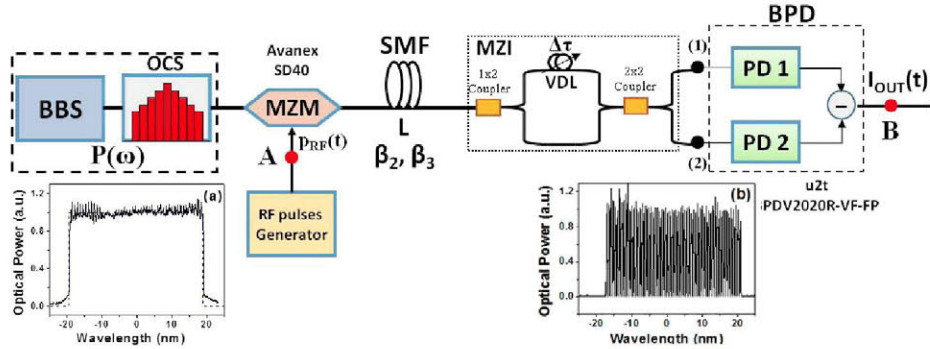

Fig. 1. Experimental setup of chirped microwave pulse generator by means of non-linear dispersion-based incoherent photonic processing. Inset (a) optical source power spectral distribution. Inset (b) optical signal spectrum at point (1) of the system.

Following an analysis similar to [19], we can find that the photodetected current at the output of each MZI branch corresponds to the following expression:

$$I_{out}^{(1)}(t) = r(t) \cdot \frac{\alpha}{2} [1 + V \cos(\Delta \tau \cdot \omega)]_{\omega = \omega_{rf}(t)} \qquad I_{out}^{(2)}(t) = r(t) \cdot \frac{\alpha}{2} [1 - V \cos(\Delta \tau \cdot \omega)]_{\omega = \omega_{rf}(t)} \quad (2)$$

where α corresponds to the propagation losses of each arm and V is the visibility of the interference in the MZI response. From the analysis of Eq. (6) in [19], we can obtain that the nonlinear operation regime implies to satisfy the condition $\sigma_0 << \delta\omega^2\beta_3L$, where σ_0 and $\delta\omega$ the RF pulse time duration and the optical source bandwidth, respectively. Equation (2) shows that this approach permits to generate an envelope $r(t)$ completely described in [19] with a proportional dependence on the optical source power distribution modified by a scale factor between the optical frequency ω and the instantaneous angular frequency $\omega_{rf} = 2\pi f_{rf}$. Besides, note the complementary responses of the photocurrents $I_{out}^{(1)}(t)$ and $I_{out}^{(2)}(t)$ due to the both complementary optical transfer functions of both MZI outputs. In this way, the resultant photocurrent for the generated waveform after the BPD is given by $I_{out}(t)$:

$$I_{out}(t) = I_{out}^{(1)}(t) - I_{out}^{(2)}(t) = r(t) \cdot \alpha V \left[\cos(\Delta\tau \cdot \omega) \right]_{\omega = \omega_{rf}(t)} \quad (3)$$

In this paper, we focus our attention in the second term of Eq. (3). Note that the baseband component is removed comparing to the theoretical structure without differential detection [19]. This is the key point which permits to obtain high values of SNR simplifying the averaging process needed when a system operates in incoherent regime [20]. In this way, the second term provides the instantaneous frequency $\omega_{rf} = 2\pi f_{rf}$ of the generated pulse which can be written as (Eq. (9) of [19]):

$$f_{rf}(t) = \frac{f_0}{\sqrt{1 + 2\frac{\beta_3 L}{(\beta_2 L)^2} t}} \approx f_0 + \frac{t}{C} \quad (4)$$

In Eq. (4), we have included a linear approximation by the first order Taylor polynomial which permits to show the relationship between the instantaneous frequency and the chirp C.

The central frequency f_0 and the chirp C are given by:

$$f_0 = \frac{\Delta\tau}{2\pi(\beta_2 L)} \qquad C = -\frac{\beta_2}{f_0\beta_3}(\beta_2 L) \quad (5)$$

These two parameters, frequency f_0 and chirp C, are key to fully exploit the system capabilities as shown in the next section. According to Eq. (5), firstly, the fiber link length (L) is selected to obtain a particular chirp value. Then, design central frequency of the waveform is achieved by the proper adjustment of the time delay of the MZI by the VDL. In order to show the system performance, we select an optical source uniform profile with a 3-dB bandwidth of 38.4 nm. Inset (a) of Fig. 1 plots the optical profile measured with an optical spectrum analyzer (Yokogawa AQ6370C). Following with the previous experimental conditions described in Fig. 1, we consider a fiber link of L = 10 km and a MZI time delay Δτ = 7 ps. In this way, the central frequency is fixed around 5 GHz and the chirp is 6.91 ns/GHz according to Eq. (5). The optical power between two MZI arms has been balanced through an optical attenuator. Inset of Fig. 1(b) plots the optical signal spectrum at point (1) of the system, showing a high visibility (> 20 dB).

Figure 2(a) shows the spectrum of the generated pulse whose envelope corresponds to the theoretical prediction included in dashed line showing a good agreement. The corresponding generated waveform is plotted in Fig. 2(b). The T_{FWHM} is 6.5 ns and its envelope is according to the profile of the optical source as it is expected from the envelope r(t) [19]. Instantaneous frequency, f_{rf}, is plotted by means of points (●) in Fig. 2(c), which is calculated inverting the time period of the experimental signal measured with the sampling oscilloscope. As observed,

the instantaneous frequency has a variation or chirp along the generated signal. The variation of the instantaneous frequency is almost linear and goes from 4.6 to 5.5 GHz. Therefore, in this case, the generated waveform has a TBWP = 7.3. Note that Fig. 2 includes theoretical predictions in dashed lines showing a good agreement with experimental results.
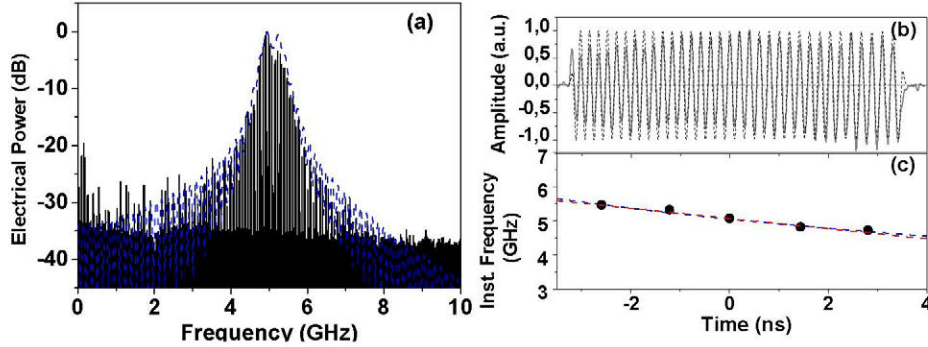

Fig. 2. (a) Spectrum of the generated signal and theoretical predictions included in dashed blue lines. (b) Generated waveform (black solid line) and theoretical simulation (black dashed line). (c) Instantaneous RF frequency (●) and its theoretical prediction (blue dashed line) and linear approximation (red dashed line).

Finally, it is important to distinguish between our previous contribution [7] and this novel proposal. The main difference is focused on the use of the linear ($\beta_3 = 0$) or non-linear ($\beta_3 \neq 0$) properties of the dispersive element. In this novel approach, the use of larger fiber lengths and wider optical sources leads to a totally different operation regime in order to strategically exploit the dispersion slope β_3 in the waveform generation. In this way, the condition assumed in Eq. (2) is satisfied for all the cases shown through this paper. In fact, this nonlinear contribution was negligible in [7]. Therefore, this manuscript corresponds to the first-ever experimental demonstration of the chirped waveform generation by means of the incoherent optical processing by nonlinear dispersive elements.

3. Experimental capabilities

In order to experimentally show the system capabilities, different chirped pulses were generated controlling the power spectral density of the optical source, dispersion and time delay difference through OCS, fiber link length and MZI, respectively.

A TBWP control is achieved through the dispersion of the system, specifically, through the nonlinear dispersive element which corresponds to the fiber link. Fig. 3 shows a chirped pulse generated with a uniform envelope.

In this case, the fiber link is changed by one of L = 20 km and the time delay difference introduced by MZI is set to $\Delta\tau$ = 13.6 ps. The electrical spectrum (measured and simulated) of the generated signal are plotted in Fig. 3(a). Controlling the VDL of the MZI according to Eq. (5), the central frequency is still around 5 GHz. Fig. 3(b) shows the generated waveform, with a T_{FWHM} of 12.8 ns, and its instantaneous frequency (●) which ranges from 4.5 to 5.5 GHz and is centered around 5 GHz achieving a TBWP = 12.8. Thereby, an increment of factor 2 in the dispersion introduced by the system leads to an increase in TBWP almost doubled than the previous case. Therefore, the TBWP parameter of a chirped pulse can be controlled by means of the first order dispersion parameter of the fiber link.
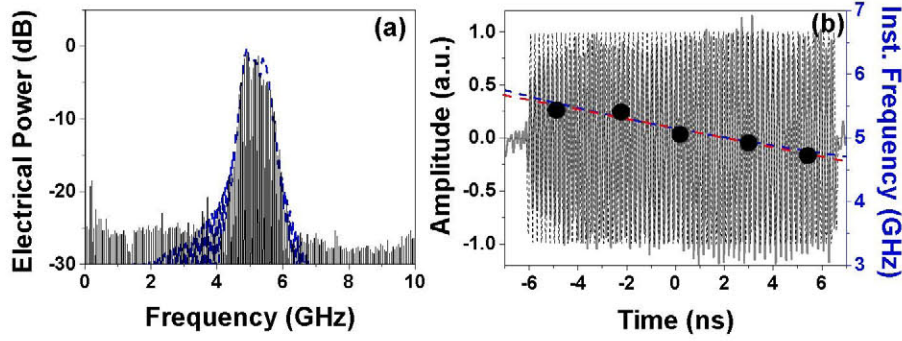
Fig. 3 (a) Measured (black solid line) and simulated (blue dashed line) electrical spectrum when 20 km fiber length is considered. (b) Experimental generated waveform (black solid line) and simulation (black dashed line). Instantaneous RF frequency (●) with theoretical prediction (blue dashed line) and linear approximation (red dashed line).

On the other hand, the system is able to change the central frequency of the generated signal by means of the adjustment of the time delay difference introduced by the MZI. In order to show this tunability, two signals with a central frequency of 10 GHz have been generated as plotted in Fig. 4. Firstly, a fiber link of L = 10 km is used and the time delay difference introduced by MZI is set to $\Delta\tau$ = 14.2 ps.
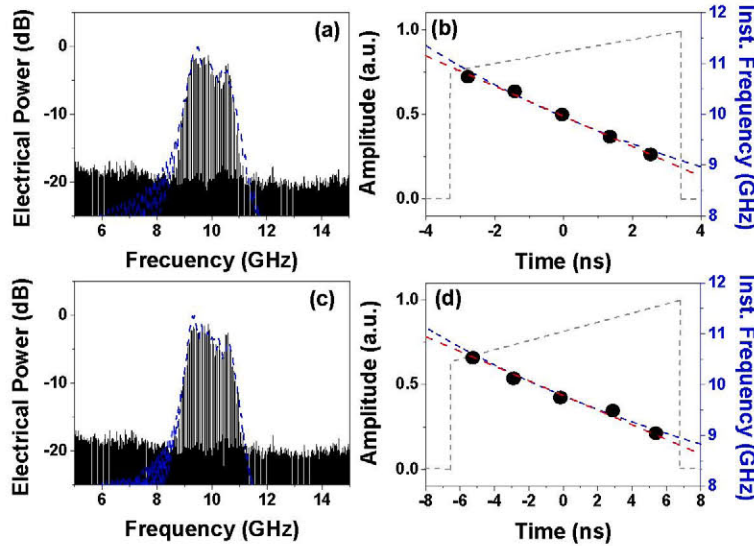

Fig. 4. Measurement of the electrical spectrum (black solid line) and simulation (blue dashed line) centered at 10 GHz considering a SMF link of (a) L = 10 km and (c) 20 km. In (b) and (d), corresponding instantaneous RF frequency (●) with its theoretical prediction (blue dashed line) and linear approximation (red dashed line). Besides, theoretical envelope of generated waveform (dashed line) is included.

Figure 4(a) shows the spectrum of the generated signal and the corresponding simulation. The frequency components of the generated pulse are around 10 GHz according to Eq. (5). Figure 4(b) shows the theoretical envelope of the generated signal. In this case, waveform measurement is not included to achieve simplicity in the Fig. 4. Indeed, its visualization is not relevant compared to the corresponding experimental instantaneous frequency (●) shown in Fig. 4(b). The experimental time duration of the signal is T_{FWHM} = 6.7 ns and its instantaneous frequency ranges from 9 to 11 GHz, leading a TBWP of 13.4. Compared with the generated signal of Fig. 3, we show that it is possible to change the central frequency of the generated

waveform from 5 to 10 GHz maintaining the value of the TBWP. Therefore, from both previous examples related to Fig. 3(b) and 4(b), we demonstrated the capability of controlling independently the TBWP and the central frequency of the generated signal. Secondly, Fig. 4(c) shows the spectrum of the generated signal when a fiber link of L = 20 km is used. The corresponding envelope of the generated signal and its instantaneous frequency (●) are plotted in Fig. 4(d). In this case, T_{FWHM} = 13.2 ns achieving a TBWP = 26.4. This value of TBWP is a significant improvement over nonlinear frequency-to-time coherent mapping approaches [13–15] where the maximum TBWP achieved is around 4.

4. Discussion

This work corresponds to an experimental evaluation of our previous theoretical proposal [19] where theoretical basis of the processing of incoherent optical signals by means of nonlinear dispersive elements is established. Moreover, we have considered the introduction of differential detection in this contribution in order to increase the SNR of the system. In this way, we experimentally have demonstrated a chirped microwave pulses generator through the processing of an incoherent optical signal by means of a nonlinear dispersive element. In the literature, different approaches using a coherent optical signals can be found. For these cases, the chirped characteristic is introduced by unbalanced temporal pulse-shaping [12], non-linear frequency-to-time mapping [13–15] or directly in the optical shaping of the coherent signal [16–18]. Our system improves considerably the TBWP of [12–15] and reaches the same order of magnitude than [16–18]. Furthermore, the system proposed is able to easily reconfigure the waveform envelope through the OCS achieving a improvement of the flexibility respect to the approaches previously mentioned.

Additionally, it is worth to emphasize the differences of this proposal and our previous work [7]. In principle, the current scheme and the approach presented in [7] are structurally similar. However, the operation regime of the current approach is totally and completely different from the previous one. Indeed, this is the key point of the novelty for this manuscript. As previously mentioned, the condition $\sigma_0 << \delta\omega^2\beta_3L$ determines directly the nonlinear operation regime. The time width of the RF pulse used both in [7] and the current proposal is 80 ps. For the experimental parameters assumed in [7] that condition is not fulfilled. Indeed, the satisfied condition is opposite, i.e., $\sigma_0 > \delta\omega^2\beta_3L$ so the effects of the nonlinear dispersion are negligible. However, in the current proposal with larger fibre lengths and optical bandwidth up to 40 nm the nonlinearity condition is clearly satisfied leading to chirped pulses generation. Therefore, each proposal operates in a completely different regime despite the initial similarities between both experimental schemes.

5. Conclusion

In conclusion, we have experimentally demonstrated, for the first time, a technique for chirped microwave pulses generation based on the processing of an incoherent optical signal using a nonlinear dispersive element. Different capabilities of the system have been experimentally demonstrated as TBWP control and frequency tuning through the dispersion induced by a fibre link and the difference time delay in a MZI. In this sense, a maximum TBWP of 26.4 has been achieved which is in the same order of magnitude obtained by current optical coherent techniques. Therefore, our system exploits to achieve high TBWP as coherent techniques but showing a full flexibility due to its incoherent processing. On the other hand, the use of differential detection overcomes the limitation related to intensity noise, and thus, the number of averages required using incoherent sources is reduced.

Acknowledgments